Cell

Pluripotency Factors in Embryonic Stem Cells Regulate Differentiation into Germ Layers

Matt Thomson,[1,2,3] Siyuan John Liu,[1,6] Ling-Nan Zou,[1,3] Zack Smith,[4] Alexander Meissner,[3,4] and Sharad Ramanathan[1,2,3,5,6,*]
[1]FAS Center for Systems Biology
[2]Biophysics Program
[3]Harvard Stem Cell Institute
[4]Department of Stem Cell and Regenerative Biology
[5]School of Engineering and Applied Sciences
[6]Department of Molecular and Cellular Biology
Harvard University, Cambridge, MA 02138, USA
*Correspondence: sharad@post.harvard.edu
DOI 10.1016/j.cell.2011.05.017

SUMMARY

Cell fate decisions are fundamental for development, but we do not know how transcriptional networks reorganize during the transition from a pluripotent to a differentiated cell state. Here, we asked how mouse embryonic stem cells (ESCs) leave the pluripotent state and choose between germ layer fates. By analyzing the dynamics of the transcriptional circuit that maintains pluripotency, we found that Oct4 and Sox2, proteins that maintain ESC identity, also orchestrate germ layer fate selection. Oct4 suppresses neural ectodermal differentiation and promotes mesendodermal differentiation; Sox2 inhibits mesendodermal differentiation and promotes neural ectodermal differentiation. Differentiation signals continuously and asymmetrically modulate Oct4 and Sox2 protein levels, altering their binding pattern in the genome, and leading to cell fate choice. The same factors that maintain pluripotency thus also integrate external signals and control lineage selection. Our study provides a framework for understanding how complex transcription factor networks control cell fate decisions in progenitor cells.

INTRODUCTION

How progenitor cells decide their fate is a question that underlies all of developmental biology but is poorly understood. While complex regulatory networks are known to maintain cells in distinct cell fates (Davidson et al., 2002; Novershtern et al., 2011; Odom et al., 2004), we know little about how cells integrate signals and reorganize these networks to allow fate transitions.

Mouse embryonic stem cells (ESCs) provide a model system for studying cell fate choice (Nishikawa et al., 2007; Niwa, 2010). The cells integrate signals in their environment and choose whether to remain pluripotent or to differentiate into progenitors of the mesendoderm (ME) or neural ectoderm (NE) (Figure 1A) (Greber et al., 2010; Nishikawa et al., 2007; Niwa, 2007, 2010; Niwa et al., 2000; Tesar et al., 2007; Yamaguchi et al., 1999; Ying et al., 2003b). A complex circuit of transcription factors and epigenetic regulators (including Oct4, Sox2, Nanog, Klf4, Klf5, Tbx3; Jarid2, Suz12) holds the ESC in a pluripotent state (Figure 1B) by repressing genes required for ME and NE differentiation (Ema et al., 2008; Han et al., 2010; Jiang et al., 2008; Pasini et al., 2010; Peng et al., 2009; Schuettengruber and Cavalli, 2009; Silva and Smith, 2008). High-throughput experiments have provided a complex but static picture of the pluripotency circuit (Chen et al., 2008; Lu et al., 2009; Marson et al., 2008; Wang et al., 2006) (a part of which is shown in Figure 1B), but we do not know how an ESC leaves the pluripotent state and selects between the ME and NE cell fate.

Since pluripotency circuit expression is sufficient to block all differentiation (Kim et al., 2008; Mitsui et al., 2003; Takahashi and Yamanaka, 2006), the circuit must be reorganized during germ layer differentiation so that cells can release the gene expression program associated with either ME or NE lineage. Here, we study the dynamic regulation of pluripotency circuit components during in vitro differentiation to gain insight into the regulatory mechanisms underlying cell fate selection in this system.

By analyzing circuit dynamics during lineage selection, we are able to disentangle the complex network (Figure 1B) and focus on key factors that both regulate pluripotency and control germ layer differentiation. While most pluripotency circuit factors are downregulated or variably expressed during differentiation, Oct4 and Sox2 are not. Oct4 is upregulated in cells choosing the ME fate but repressed in cells choosing the NE fate. Conversely, Sox2 protein level is upregulated in cells choosing the NE and repressed in those choosing the ME fate. Oct4 and Sox2 protein levels provide continuous temporal markers of the cell's progression toward lineage selection before lineage specific markers are activated. The lineage specific regulation

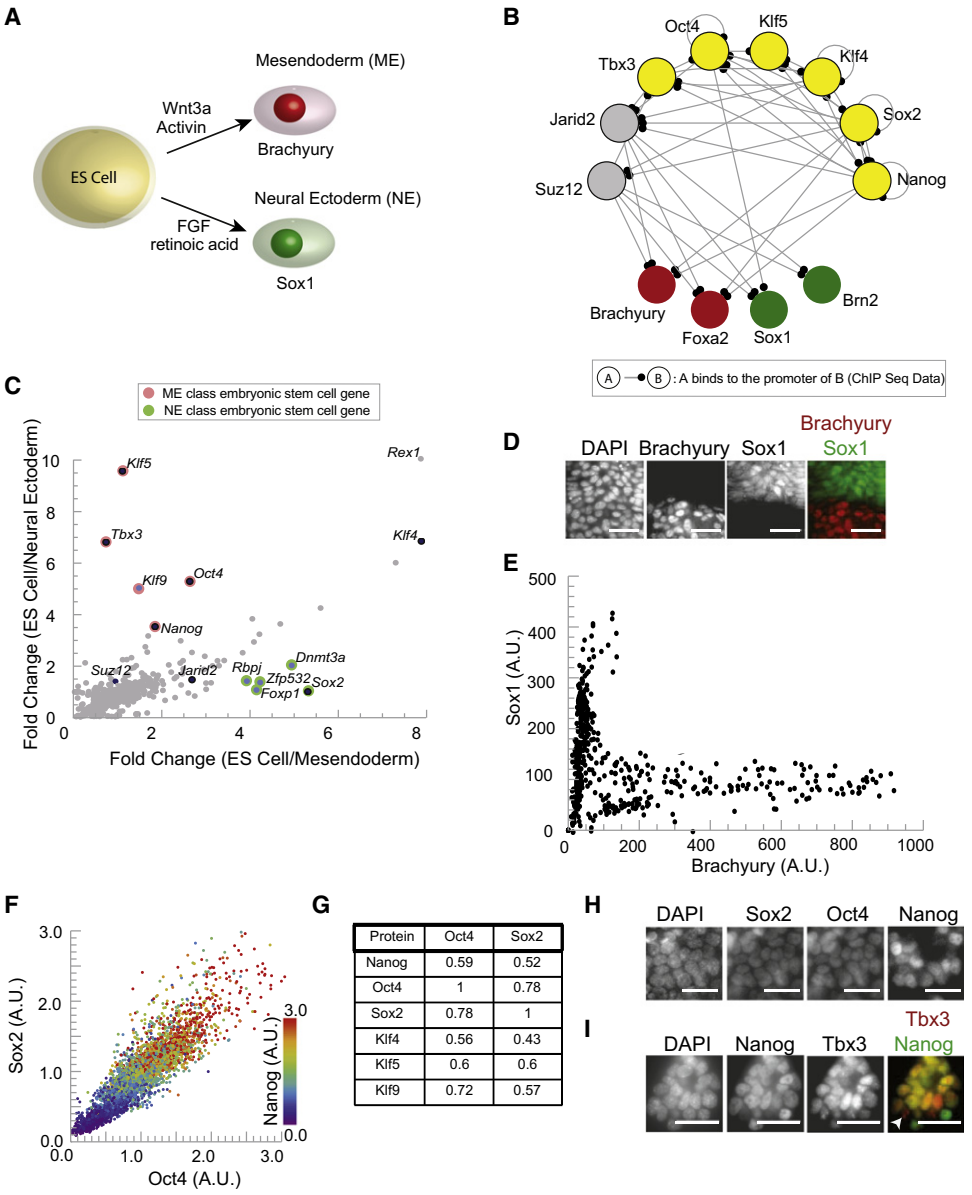

Protein	Oct4	Sox2
Nanog	0.59	0.52
Oct4	1	0.78
Sox2	0.78	1
Klf4	0.56	0.43
Klf5	0.6	0.6
Klf9	0.72	0.57

Figure 1. ESCs, Defined by Correlated Expression of Pluripotency Factors, Select between NE and ME Fate In Vitro

(A) ESCs lose pluripotency and differentiate into ME progenitor cells to express Brachyury in response to Wnt3a or Wnt agonist, CHIR. They differentiate into NE progenitors to express Sox1 in response to FGF signals or retinoic acid.

(B) Diagram of interactions between the pluripotency factors (yellow), key epigenetic regulators (gray), and regulators of the ME (red) and NE (green) lineage inferred from ChIP-seq data in the literature.

(C) Plot of fold change in expression levels (obtained from microarray data in Shen et al. [2008]) of genes expressed in ESCs compared to their expression in ME progenitors (x axis) versus the same fold change comparison in NE progenitors (y axis). Pluripotency factors and key epigenetic regulators are indicated with black dots, ME class genes in red, and NE class genes in green.

(D) Fluorescence images of Sox1-GFP ESCs exposed to 3 μM CHIR and stained with DAPI and immunostained for Brachyury show cytoplasmic GFP expression (green, NE marker) or nuclear Brachyury expression (red, ME marker). Scale bars represent 32 μm.

(E) Scatter plot of Sox1 levels versus Brachyury levels in differentiated cells. Each point represents Brachyury and Sox1-GFP signal in a single cell.

(F) Scatter plot of protein levels in single cells for Oct4, Sox2, and Nanog derived from immunofluorescence measurements for n > 1000 ESCs growing in LIF and BMP. Protein levels measured in units normalized to the population mean. Figure S1F shows population distributions of Oct4 and Sox2 protein levels.

(G) Pearson correlation coefficients for pairs of pluripotency factors measured using immunofluorescence and FACS.

(H) Fluorescence images of ESC nuclei stained simultaneously for DAPI, Sox2, Oct4, and Nanog. Scale bars represent 32 μm.

(I) Fluorescence images of ESCs stained for DAPI, Nanog and Tbx3. White arrow points to punctate Tbx3 expression (red) in a nucleus with low Nanog (green). Intensity of the delocalized nuclear Tbx3 and Nanog have a correlation of R = 0.65. Scale bars represent 32 μm.

See also Figure S1.

of Oct4 and Sox2 is necessary for germ layer fate choice and alters their binding pattern in the genome. The intimate involvement of these key nodes of the pluripotency circuit in initiating differentiation enables the cell to integrate signals and choose between different fates.

RESULTS

Gene Expression Patterns Define Three Classes of ES Factors

We identified transcription factors and DNA binding proteins that are expressed in ESCs and studied their regulation in ME and NE progenitor cells (Figure 1C) using published microarray data (Shen et al., 2008). We found that many genes (diagonal points in Figure 1C) present in the ESC are downregulated in both ME and NE cells, including *Klf4*, a pluripotency circuit factor, and *Rex1*, a commonly used ESC marker (Masui et al., 2008) (see the Extended Experimental Procedures available online). However, several genes were present in the ESC and differentially present in either ME or NE progenitors and fell near either axis in Figure 1C.

We identified a class of genes that was expressed in ESC and ME progenitors but specifically downregulated in NE progenitor cells (Figure 1C, red points). This ME class of genes contained the pluripotency genes *Oct4*, *Nanog*, *Klf5*, *Tbx3*, and *Klf9*. Complementarily, a class of genes, we call the NE class, was expressed in ESCs and in NE progenitor cells but downregulated in ME progenitor cells (Figure 1C, green points). This class contained the pluripotency circuit gene *Sox2*, as well as *Foxp1*, *Rbpj*, *Dnmt3a*, and *Zfp532*. We classified genes as belonging to the ME or NE class based upon their distance from the diagonal in Figure 1C (a table with distances and p values is in Figure S1C; see the Extended Experimental Procedures for details). Surprisingly, many of the core pluripotency circuit genes, including *Nanog*, *Oct4*, *Sox2*, *Klf5*, and *Tbx3*, had signatures of lineage specific regulation, suggesting a deeper connection between pluripotency maintenance and lineage choice.

We then developed an experimental system for studying the expression of the ME and NE class genes during lineage choice in single cells.

ESCs Differentiate into Germ Layer Progenitors In Vitro

We reconstituted the NE versus ME cell fate decision in vitro and established an experimental system in which we could differentiate a cell population into either the ME or NE lineage by adding Wnt or retinoic acid.

We maintained ESCs in the pluripotent state using LIF and BMP in defined conditions without serum or feeder cells using methods described previously (Ying et al., 2003a; Ying et al., 2008) (Extended Experimental Procedures). Cells removed from pluripotency promoting conditions did not immediately respond to NE or ME inducing signals, and this effect has been reported in the literature (Jackson et al., 2010). However, after 48 hr in N2B27, a defined medium that lacks differentiation signals (Extended Experimental Procedures), cells became competent to respond to signals.

After 48 hr in N2B27, cells responded to Wnt3a or CHIR, a Wnt agonist, by activating the core mesendodermal regulators Brachyury and Foxa2 (Figure 1D and Figure S1D), with more than 70% of cells expressing Brachyury within 36 hr of signal addition at high levels of signal (e.g., 3 μM CHIR). After 48 hr in N2B27, retinoic acid (RA) or FGF drove NE differentiation and triggered the activation of NE markers, Sox1, Brn2, and Nestin (Figure 1D and Figure S1E). Consistent with the published literature, 70% of cells activated Sox1 within 36 hr of signal addition (Abranches et al., 2009; Ying et al., 2003b). In this way, Wnt or retinoic acid signals drove high-efficiency differentiation of ESCs to the ME or NE cell fate, respectively.

Even in the presence of Wnt3a or CHIR, a population of cells activated Sox1, the NE regulator, and not Brachyury, the ME regulator. This is presumably due to the paracrine FGF signaling between the cells leading some cells to adopt the NE fate (Ying et al., 2003b). Using a previously validated Sox1-GFP reporter cell line (Ying et al., 2003b) and Brachyury immunofluorescence, we could detect Sox1 and Brachyury activation in the same cell population (Ying et al., 2003b). In cell populations treated with Wnt3a or CHIR, Sox1-GFP expression and Brachyury staining were mutually exclusive (Figures 1D and 1E). There are no points on the diagonal of the scatter plot in Figure 1E, illustrating the absence of simultaneous high Sox1 and Brachyury expression in single cells. The "L" shape of the scatter plot shows that cells make a discrete decision to activate either Sox1 or Brachyury in vitro.

Our ability to induce and detect Sox1 positive and Brachyury-positive cells under identical conditions provided a defined experimental system for studying the regulation of the pluripotency circuit factors during ME versus NE lineage selection. We validated the differentiation protocol with a variety of cell lines.

Nanog Downregulation Is Necessary for Lineage Selection

We used immunofluorescence to measure the levels of the proteins identified in Figure 1C in single cells as we took the cells through the differentiation protocol described in the previous section. We performed immunofluorescence staining under identical conditions in all experiments so that protein levels could be quantitatively compared between different cell populations (Sachs et al., 2005).

Consistent with the dense network of positive regulatory interactions that have been inferred between pluripotency factors (Chew et al., 2005; Ivanova et al., 2006; Masui et al., 2007), in populations of cells growing under pluripotency promoting conditions, pluripotency circuit protein levels were strongly correlated across the cell population (Figures 1F–1I).

Cells responded to differentiation signals only 48 hr after the withdrawal of pluripotency-promoting conditions (Figure 2A). After 48 hr in N2B27, microarrays showed that 87% of genes changed by less than 2-fold, while 9% (including many pluripotency factors) were downregulated by more than 2-fold, and 4% were induced by more than 2-fold after 48 hr, as shown by the histogram in Figure 2B. *Nanog*, *Oct4*, *Sox2*, *Klf4*, *Klf5*, and *Tbx3* messenger RNA (mRNA) levels were 5%, 74%, 30%, 14%, 19%, and 12% of their levels in ESCs (Figure 2B). A small number of genes were induced, including *Dnmt3b* (Figure 2B) (Lu et al., 2009). Dnmt3b is a de novo DNA methyltransferase that

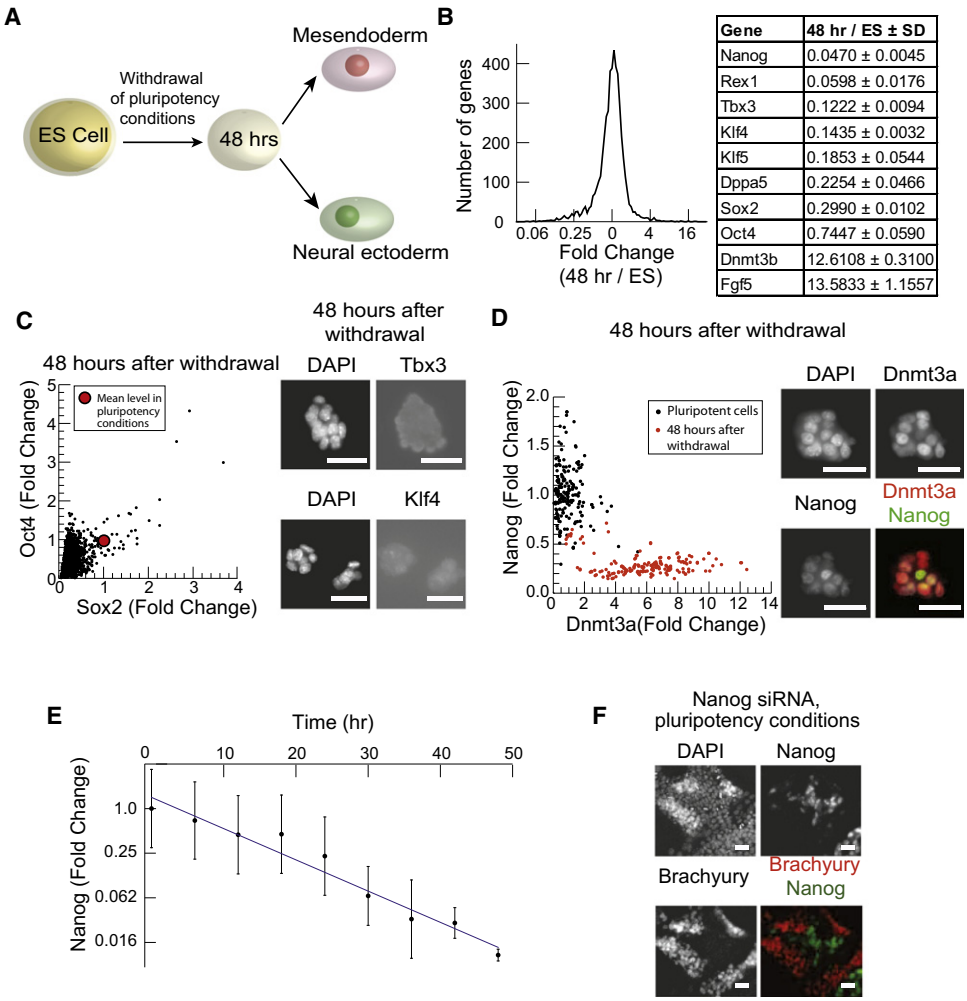

Gene	48 hr / ES ± SD
Nanog	0.0470 ± 0.0045
Rex1	0.0598 ± 0.0176
Tbx3	0.1222 ± 0.0094
Klf4	0.1435 ± 0.0032
Klf5	0.1853 ± 0.0544
Dppa5	0.2254 ± 0.0466
Sox2	0.2990 ± 0.0102
Oct4	0.7447 ± 0.0590
Dnmt3b	12.6108 ± 0.3100
Fgf5	13.5833 ± 1.1557

Figure 2. Downregulation of ESC-Specific Factors Is Necessary for Differentiation

(A) Schematic of ESC differentiation protocol. 48 hr after the withdrawal of pluripotency promoting conditions (LIF and BMP), cells are exposed to differentiation signals. Cells then respond to ME inducing signals (Wnt3a or CHIR) by activating Brachyury and to NE inducing signals (retinoic acid or endogenous FGF) by activation of Sox1.

(B) Histogram of fold change of mRNA expression levels in the cell population 48 hr after withdrawal of LIF and BMP as measured by microarray. The table shows fold changes for a set of pluripotency factors as well as for *Dnmt3b* and *Fgf5*.

(C) The scatter plot (left) of Oct4 versus Sox2 expression in n > 1000 single cells 48 hr after withdrawal of pluripotency conditions. The red dot indicates mean expression level of these proteins in pluripotency conditions. Fluorescent images (right) of cells immunostained for DAPI, Tbx3 (above) and Klf4 (below) 48 hr after withdrawal of pluripotency conditions. Scale bars represent 32 μm.

(D) Scatter plot of Nanog versus Dnmt3a levels in single cells under pluripotency supporting conditions (black) and 48 hr after the withdrawal of pluripotency conditions (orange). Images of cells immunostained for DAPI, Dnmt3a (red) and Nanog (green) 48 hr after pluripotency condition withdrawal are shown. Scale bars represent 32 μm.

(E) Plot of the fold changes of mean Nanog protein levels (>20,000 cells) in cell populations fixed every 6 hr after withdrawal of LIF and BMP. Error bars indicate ± standard deviation (SD) in Nanog protein levels in the cell population. Solid line shows Nanog decay fit to an exponential with a half-life of 7.5 hr.

(F) Fluorescence images of cells in pluripotency conditions, LIF and BMP, stained for DAPI, Nanog, and Brachyury after CHIR addition for 24 hr and siRNA knockdown of Nanog. siRNA construct was added to cells for 24 hr prior to CHIR exposure. Scale bars represent 32 μm.

See also Figure S2.

acts with Dnmt3a to methylate the promoters of the pluripotency circuit factors including *Nanog* during germ layer differentiation (Li et al., 2007).

Consistent with the microarray data, the protein levels of Oct4, Sox2, Nanog, Klf4, Klf5, Tbx3, and Klf9 fell during the transition, while Dnmt3a and Dnmt3b were induced up to 3-fold (Figures 2C and 2D and Figure S2A). In Figure 2C, the mean levels of Oct4 and Sox2 in more than 99% of the cells are below the mean expression levels of these proteins in pluripotency supporting conditions. Cell images (Figure 2C) show that Tbx3 and Klf4 protein levels are severely downregulated upon withdrawal of pluripotency sustaining conditions (compare Figure S2A).

Thus, while in ESCs Nanog is expressed at high levels and Dnmt3a at low levels (black scatter plot in Figure 2D), after 48 hr, the cells show a complementary pattern of expression with high levels of Dnmt3a and low levels of Nanog (red scatter plot in Figure 2D; images in Figure 2D), consistent with an antagonistic regulatory relationship between these factors (Li et al., 2007).

Next, we asked whether a fall in Nanog levels might drive the ESC into the responsive state. We found that the mean Nanog protein level in the cell population fell exponentially in time (half-life 7.5 hr) by 100 fold after 48 hr in N2B27 (Figure 2E), suggesting that Nanog downregulation might be an early and causal event for driving the ESC into the responsive state.

Consistently, short interfering RNA (siRNA)-mediated knockdown of Nanog in ESCs growing in pluripotency promoting conditions led to a correlated decrease in Oct4 and Sox2 protein levels (Figure S2). Further, in these conditions, CHIR drove Brachyury activation only in cells that had lost Nanog (Figure 2F). In the presence of Nanog, activation of the Wnt pathway with CHIR or other pathway agonists is known to promote pluripotency (Sato et al., 2004; Ying et al., 2008). Thus, Nanog knock down was necessary and sufficient for Brachyury activation by CHIR.

Oct4 and Sox2 Are Differentially Regulated during Fate Choice

The correlated expression pattern of the pluripotency factors in ESCs (Figure 1F) contrasts sharply with the lineage-specific expression pattern that we observed in our microarray analysis (Figure 1C). We asked whether this change in correlation pattern is reflected in protein levels of pluripotency factors in individual cells during differentiation.

After 48 hr of pluripotency condition withdrawal (LIF and BMP), cells were not committed to a lineage and could be driven to either cell fate by signal addition (Figure 2A). We added differentiation signals to cells 48 hr after withdrawal of pluripotency conditions. Upon addition of signal (3 μM CHIR, Figures 1D and 1E), some cells adopted the ME (Brachyury expression) and others the NE (Sox1 expression) lineage.

We studied the regulation of genes in the ME class (*Oct4*, *Nanog*, *Klf5*, *Tbx3*, and *Klf9*) and NE class (*Sox2*, *Foxp1*, *Dnmt3a*, *Rbpj*, and *Zfp532*) defined above to ask how the pluripotency circuit is regulated during lineage selection. In addition to the ME and NE class, we studied the pluripotency factor, *Klf4*, and the key epigenetic regulator, *Jarid2*, which controls the targeting of repressive epigenetic modifications to the genome in pluripotent and differentiating ESCs (Peng et al., 2009).

Of the genes identified from the microarray analysis as belonging to the ME or NE class, Tbx3, Klf4, Klf9, and Rbpj proteins were absent or present at very low levels in cells entering both the NE and ME lineages and were not reactivated during differentiation (Figure 2C and Figure S3). This suggests that these factors play a role in pluripotency maintenance but not in lineage choice. In contrast, Oct4, Sox2, Nanog, Jarid2, Klf5, Foxp1, and Dnmt3a proteins were present in the nucleus of differentiating cells (Figure 3), and we classified these factors into groups based on their expression pattern.

Oct4 and Klf5 constituted the first group of proteins (Figures 3A and 3B). Oct4 protein was present exclusively in Brachyury-positive (ME) cells but absent in Sox1-positive (NE) cells. Consistently, scatter plots of the protein levels of Oct4 versus Brachyury in single cells correlated positively (Figure 3A, red scatter plot). The scatter plots of Oct4 versus Sox1 levels showed that cells with Sox1 have very low levels of Oct4 (Figure 3A, green scatter plot). Klf5 had a similar pattern of protein expression to Oct4. However, rather than being absent in Sox1-positive cells, Klf5 was confined to a subcellular compartment distinct from the nucleus (Figure 3B).

The second group of proteins included only Sox2, which was expressed in a complementary pattern to Oct4 and Klf5 (Figure 3C). In cells undergoing ME differentiation, Sox2 and Brachyury were mutually exclusive (Figure 3C, red scatter plot). In contrast, Sox2 and Sox1 (NE marker), expression correlated strongly during NE lineage induction (Figure 3C, green scatter plot).

As the final class of factors, Foxp1, Nanog, Dnmt3a, and Jarid2 were present variably in cells that had activated either Sox1 or Brachyury (Figures 3D–3G). For example, scatter plots of Dnmt3a protein levels quantify this observation and illustrate that the distribution of Dnmt3a protein is similar in both in Sox1 and Brachyury expressing cells (Figure 3F).

We quantified the data in the scatter plots by measuring the probability of observing a given protein conditioned on the presence of each lineage marker (Figure 3H and the Extended Experimental Procedures). On this plot, variably expressed proteins like Dnmt3a lie on the diagonal and are present with high probability in both Sox1 and Brachyury-expressing cells. Lineage specific proteins like Oct4 and Sox2 fall on the extreme off-diagonal of the plot and are present with high probability in either ME or NE progenitor cells but not both, consistent with the images in Figures 3A and 3C (see the Extended Experimental Procedures).

To determine whether the above patterns were established prior to lineage choice, we used FACS and live-cell imaging to study the dynamics of protein regulation in response to signal. We did not study *Klf5* further because *Klf5* knockout ESC lines can differentiate into all three germ layers (Ema et al., 2008).

Differential Modulation of Oct4 and Sox2 Levels Precedes Cell Fate Selection

We asked how the relative levels of Oct4 and Sox2 protein change in time during ME and NE differentiation. We added CHIR or RA to cell populations to induce ME or NE differentiation as described (Experimental Procedures), and determined the levels of both factors in individual cells ($n > 40{,}000$) using FACS.

After CHIR addition, the mean level of Sox2 protein fell by 72% after 8 hr and by 77% at 12 hr (Figure 4A). The mean Oct4 protein level, on the other hand, fell by 5% over the first 12 hr. At 12 hr after CHIR addition, 42% of cells had activated Oct4 to levels greater than the mean level in the cell population prior to signal addition, while only 1.7% of cells had Sox2 protein levels exceeding the Sox2 mean in the initial cell population. After 12 hr, the fold change in relative Oct4 and Sox2 protein levels differed by more than the sum of the standard deviations of either protein in the cell population. The activation of ME regulator Brachyury occurred between 12 and 15 hr after CHIR addition. By 24 hr, Oct4 levels were upregulated and Sox2 repressed in cells that had activated Brachyury (Figure 4A) as shown in the

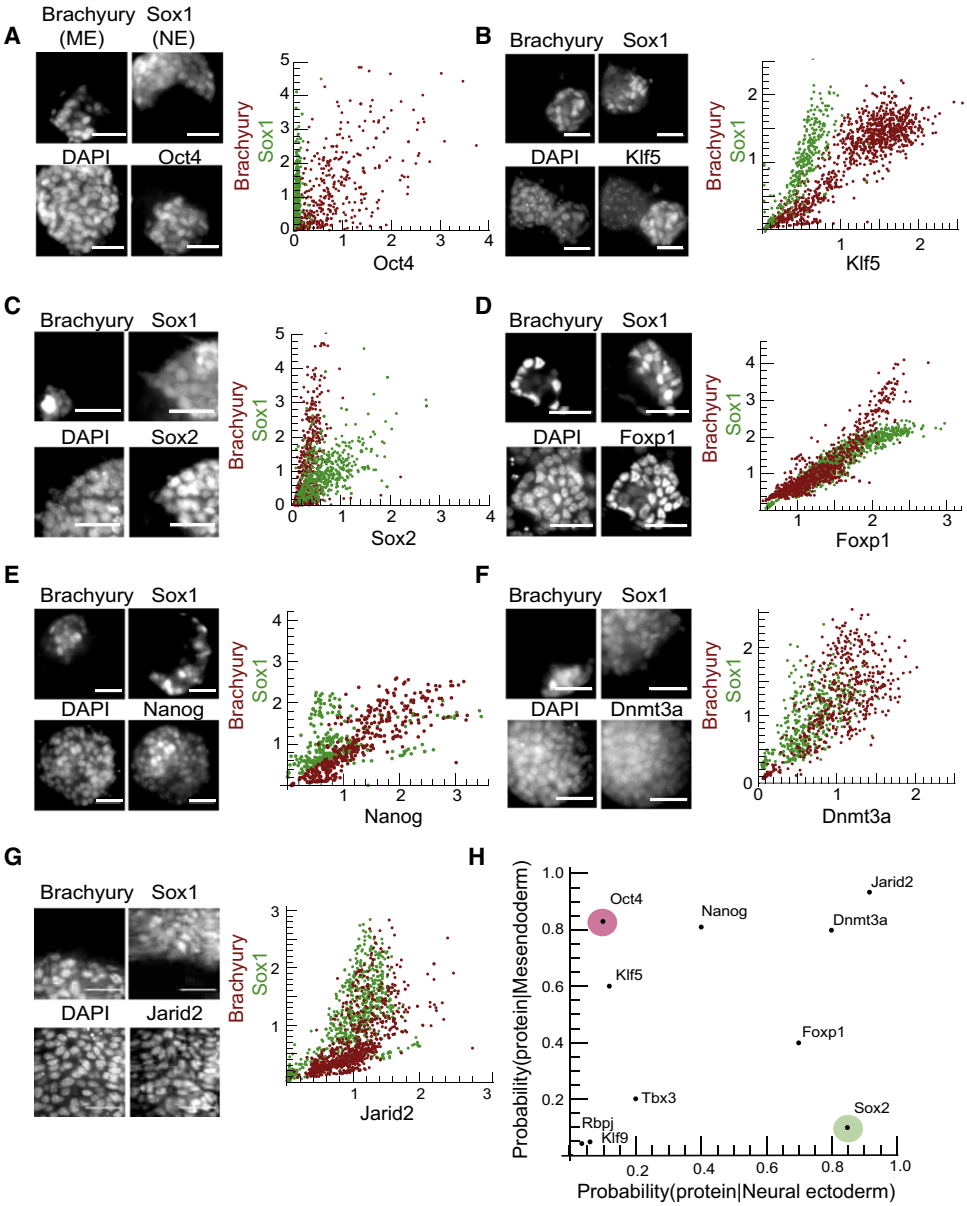

Figure 3. Key ESC Transcription Factors Are Differentially Expressed in ME and NE Cells

(A–G) Cells were differentiated in conditions (see the Experimental Procedures) where some cells adopted the ME fate (Brachyury positive) and others adopted the NE fate (Sox1-GFP positive). Images of a field of cells immunostained 36 hr after signal addition for ME marker Brachyury, NE marker Sox1, DAPI, and a specific factor (left) are shown. Scatter plots (right) are of the expression level of that factor against Brachyury in n > 300 Brachyury-positive cells (red points) and against Sox1, n > 300 Sox1-positive cells (green points) for Oct4 (A), Klf5 (B), Sox2 (C), Foxp1 (D), Nanog (E), Dnmt3a (F), and Jarid2 (G). All scale bars represent 32 μm.

(H) The data from (A)–(G) are summarized in a conditional probability plot. Each point in the plot represents the probability of finding the expression of the specific protein in ME progenitors (y axis) versus NE progenitors (x axis).

See also Figure S3.

scatter plot in Figure 4A, where cells adopting the ME fate showed high Oct4 and low Sox2 expression.

After RA addition, Oct4 and Sox2 protein levels diverged but on a longer time scale than after CHIR addition (Figure 4B). At 14 hr after RA addition, the mean level of Sox2 protein had fallen by 5% while Oct4 had fallen by 56%. At 18 hr, Sox2 protein levels were 100% of their initial level while Oct4 had fallen by 64%. At the same time point, 37% of cells had Sox2 levels greater than the mean level in the cell population prior to signal addition, while less than 1% of cells had Oct4 levels exceeding the mean in the initial cell population. At 18 hr, the relative fold change in Oct4 and Sox2 differed by more than the sum of the standard

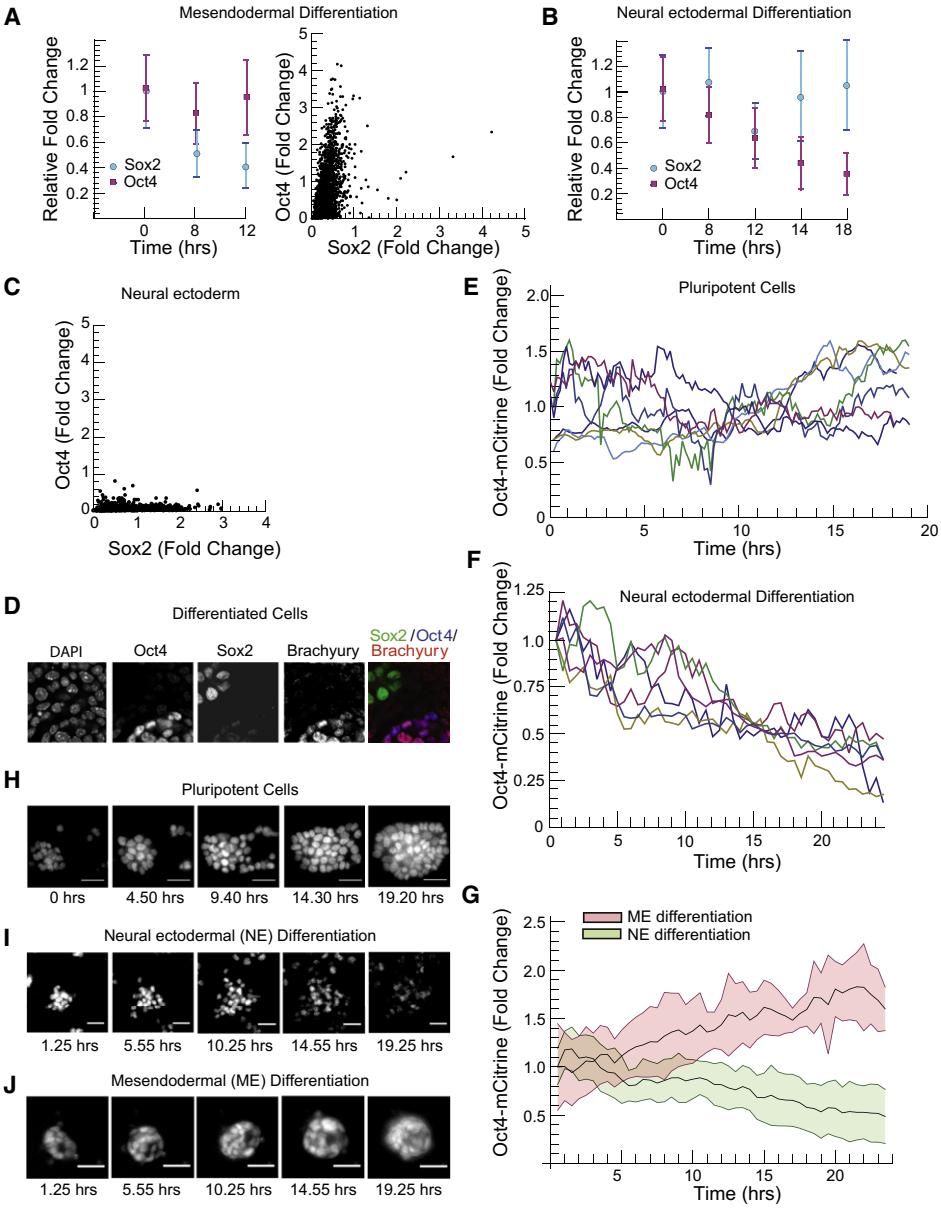

Figure 4. Oct4 and Sox2 Protein Levels Diverge Continuously during Lineage Selection

(A) Left: Plot of mean ± SD of Oct4 (purple squares) and Sox2 (blue circles) protein levels in n > 40,000 cells at 0, 8, and 12 hr after CHIR addition, measured simultaneously in single cells via immunofluorescence and FACS. Protein levels were normalized to the mean protein level in the cell population prior to signal addition. Right: Scatter plot of Oct4 and Sox2 protein levels 24 hr after signal addition in single ME progenitor cells (~2400 cells), with levels normalized to the mean level of these proteins in pluripotent cells.

(B) Plot of mean ± SD of Oct4 (purple squares) and Sox2 (blue circles) levels in populations of n > 40,000 cells after RA addition.

(C) Scatter plot of Oct4 versus Sox2 protein levels in n > 2000 cells 24 hr after RA addition. Protein levels were normalized to the mean protein level in the cell population prior to signal addition.

(D) Confocal microscopy images of cells undergoing ME differentiation stained for DAPI, Oct4, Sox2, and Brachyury.

(E) Single-cell trajectories of Oct4-mCitrine levels obtained via time lapse microscopy for ESCs growing under pluripotency-promoting conditions.

(F) Single-cell trajectories of Oct4-mCitrine in cells differentiating into the neural ectodermal lineage. Conditions supporting pluripotency were removed for 48 hr, and then retinoic acid (500 nM) was added at t = 0 to induce differentiation.

(G) Temporal trajectories of Oct4-mCitrine in n > 100 cells differentiating into NE (mean in solid line, standard deviation as a light green background) and ME progenitors (mean in solid line, standard deviation as a light red background) obtained by fluorescence time-lapse microscopy of the Oct4-mCitrine cell line (t = 0 corresponds to time of signal addition, Figure 2A).

(H–J) Fluorescence images from a time lapse imaging experiment following a field of Oct4-mCitrine cells under pluripotency promoting conditions (H), during retinoic acid driven NE differentiation (I), and (during CHIR driven ME differentiation (J). Scale bars represent 32 μm.

See also Figure S4.

deviations of either protein in the cell population. The NE maker Sox1 was activated between 17 and 19 hr after RA addition. By 24 hr, Sox2 was activated and Oct4 repressed in Sox1-expressing cells as seen in Figure 4C.

Thus, after the addition of differentiation signals, Oct4 and Sox2 protein levels diverged in time, and the correlated pattern of Oct4 and Sox2 expression of the ESC (Figure 1F) broke continuously into either a high Oct4 and low Sox2 or a low Oct4 and high Sox2 pattern during differentiation (Figures 4A–4D).

To validate our FACS results, we measured Oct4 expression dynamics in single live cells during ME and NE differentiation. We created and validated (Experimental Procedures and Figure S4) (Tesar et al., 2007) an Oct4-mCitrine fusion reporter cell line (Experimental Procedures and Figure S4). We used time-lapse epifluorescence microscopy to track Oct4-mCitrine expression in hundreds of single cells both under pluripotency-promoting conditions and during differentiation. Under pluripotency-promoting conditions, Oct4 levels in single cells varied during normal rounds of cell division (Figures 4E and 4H). After 48 hr in N2B27, Oct4-mCitrine levels in single cells decreased to 60% ± 12% of ESC levels.

NE differentiation with retinoic acid drove a rapid downregulation of Oct4-mCitrine level that was detectable in single cells within 6 hr of signal addition (Figures 4F and 4I). On average, individual cells decreased their Oct4 level to half of its initial value by 16 hr after RA addition (Figure 4F). At the population level, Oct4 level decreased linearly in time (Figure 4G).

ME differentiation drove a complementary response. Cells responded to CHIR by upregulating Oct4 (Figures 4J and 4G). In the cell population, Oct4 level increased linearly in time within 6 hr of CHIR addition (Figure 4G).

In this way, cells differentiating into the ME or NE lineage showed a detectable response in Oct4 protein levels within 6 hr of signal addition, a time that is on average 10 hr before the earliest detectable lineage specific marker expression. Further, the Oct4 temporal trajectories in cells differentiated with CHIR diverged from those differentiated with RA within 6 hr (Figure 4G). These results show that the differential modulation of Oct4 occurs prior to the expression of ME or NE lineage-specific markers.

We next determined the functional roles of Oct4 and Sox2 in lineage choice. The observed Oct4 and Sox2 protein expression patterns (Figures 3A, 3C, 4A, and 4C) suggested that Oct4 might specifically inhibit the NE lineage while promoting ME differentiation and that that Sox2 might specifically inhibit ME differentiation while promoting NE lineage choice. Our analysis of published ChIP-seq data (Chen et al., 2008) provided further evidence for the asymmetric role for Oct4 and Sox2 in regulating ME and NE differentiation (Extended Experimental Procedures and Figure S5).

Oct4 and Sox2 Bind DNA in Lineage-Specific Patterns

To ask how Oct4 and Sox2 DNA binding patterns change as their relative levels are modulated during differentiation, we used ChIP-qPCR to probe the binding of Oct4 and Sox2 along five genomic regions (*Oct4*, *Sox2*, *Nanog*, *Brachyury*, and *Sox1*) in ESCs and during ME and NE differentiation. We could not obtain reproducible ChIP-qPCR results along the *Sox1* locus in ESCs, ME, or NE progenitors (see the Experimental Procedures).

We measured the spatial distribution of binding enrichment along each genomic locus using tiled qPCR primers on ChIP samples for each factor Oct4 and Sox2, in the three lineages: ES, ME and NE. Experiments were performed on three biological replicates, and in three technical replicates for each primer pair. We validated enrichment peaks of interest using multiple primers targeted to and around the region of interest.

We validated our experimental system by comparing the results of our Oct4 and Sox2 ChIP-qPCR experiments on ESCs to published ChIP-seq data (Chen et al., 2008; Marson et al., 2008). We found that Oct4 (Figures 5B, 5E, 5I, and 5L, blue bars) and Sox2 (Figures 5C, 5F, 5J, and 5M, blue bars) binding were enriched at locations previously detected in ChIP-seq experiments (Figures 5A, 5D, 5H, 5K, blue hash marks) near the genomic loci of *Nanog* (Figures 5A–5C, blue bars), *Sox2* (Figures 5D–5F, blue bars), *Oct4* (Figures 5H–5J, blue bars), and *Brachyury* (Figures 5K–5M, blue bars). The correspondence between the peaks in our ChIP-qPCR measurement and peak calls in published ChIP-seq data suggested that the ChIP-qPCR accurately reflects Oct4 and Sox2 binding.

As ESCs differentiate, Oct4 and Sox2 protein levels first fall and then are differentially regulated during ME and NE lineage selection (Figures 2 and 4). Consistent with the fall, during both ME and NE differentiation, Oct4 and Sox2 enrichment decreased at the *Nanog* promoter (Figures 5B and 5C, red bars for ME and green bars for NE lineage) and also at the −3.5 kb ES-specific regulatory region of *Sox2* (Figures 5E and 5F, red and green bars).

However, a class of regulatory sites became differentially occupied by Oct4 or Sox2 during lineage choice. In ME progenitor cells, Oct4 is induced and Sox2 downregulated (Figure 4). In these cells, Oct4 binding was enriched at the +3.7 kb regulatory region of the *Sox2* locus (red bars in Figure 5E; Figure 5G, $p = 0.0014$), while Sox2 enrichment was uniformly depleted across the entire *Sox2* locus in ME cells (Figure 5F, red bars). The +3.7 kb (downstream) site is known to regulate Sox2 expression in neural progenitor cells (Miyagi et al., 2006; Sikorska et al., 2008; Tomioka et al., 2002).

In NE progenitor cells, Sox2 is induced while Oct4 is downregulated (Figure 4). In these cells, Sox2 binding was enriched in the +3.7 kb NE regulatory region of its own enhancer, consistent with the role of this region in controlling Sox2 expression in NE cells (Figure 5F, green bar at +3700 bp from Sox2 TSS, $p = 0.0019$). Sox2 enrichment also increased at the −4.3 kB region of the *Brachyury* promoter (Figure 5M, green bar at −4250 bp from *Brachyury* TSS; Figure 5N, green line, $p = 0.0171$) where Sox2 binding was enriched in all three NE biological replicates. In ME cells, Sox2 enrichment at this locus was detected in only one of three biological replicates (Figure 5M, red bar at −4250 bp from *Brachyury* TSS; Figure 5N, red line), likely due to contaminating subpopulations of NE progenitors, and was not statistically significant ($p = 0.37$).

In this way, while many ESC-specific binding events are depleted of Oct4 and Sox2 during differentiation, a fraction of regions become differentially occupied by either Oct4 or Sox2. As Oct4 protein levels increase relative to Sox2, Oct4 binding increases in regions of the genome associated with NE

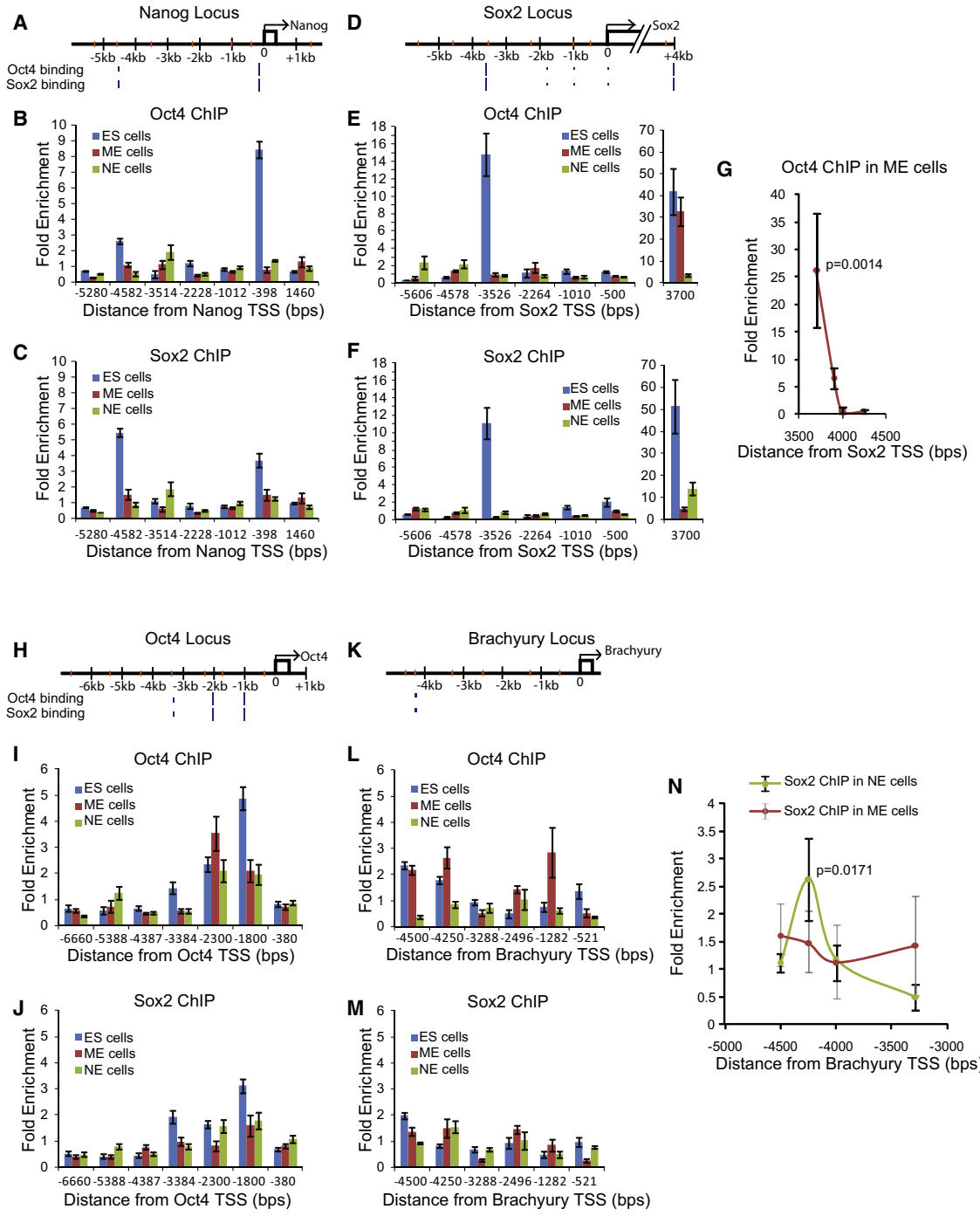

Figure 5. Oct4 and Sox2 Bind Asymmetrically in NE and ME Regulatory Regions during Differentiation

(A–N) ChIP-qPCR assays for Oct4 and Sox2 binding at *Nanog* (A–C), *Sox2* (D–G), *Oct4* (H–J), and *Brachyury* (K–N) loci in ESCs (blue bars), ME cells (red bars), and NE cells (green bars). Each genomic region is depicted with qPCR primer coordinates (orange hashes) and previously reported Oct4 and Sox2 ESC-specific binding sites (blue hashes; hash heights are proportional to published ChIP-seq peak heights). Mean fold enrichment is normalized to input, and error bars represent ± standard error of the mean (SEM) of technical triplicates. The x axis represents positions relative to the transcriptional start site.

(G) ME lineage-specific binding of Oct4 at the *Sox2* +3700 bp neural enhancer probed with multiple primer pairs. Each point and error bars represent mean enrichment values ± SEM for three biological replicates ($p = 0.0014$).

(N) Lineage-specific binding of Sox2 at the *Brachyury* −4250 bp region was probed with multiple primer pairs. Points show mean enrichment values for Sox2 in the NE lineage (green circles) and ME lineage (red circles) over three biological replicates.

Error bars (black for NE lineage, gray ME lineage) represent ± SEM of biological replicates. NE peak at −4250 bp has $p = 0.0171$, while ME enrichment has $p = 0.37$. See also Figure S5.

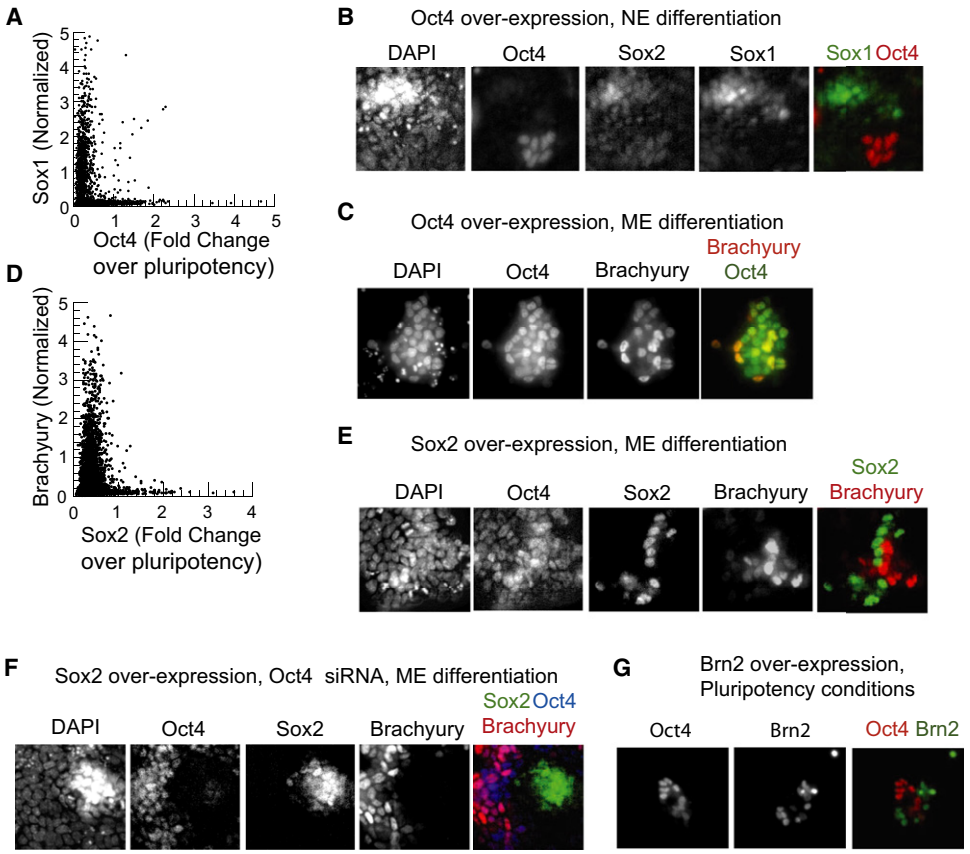

Figure 6. Oct4 Specifically Represses the NE Lineage and Sox2 the ME Lineage

(A) Scatter plot of Oct4 versus Sox1 in 2500 cells from a population in which constitutive Oct4 plasmid has been transfected and neural differentiation inducing signal retinoic acid (1 μM) was added. Oct4 levels are measured as fold change over levels in ESCs under pluripotency conditions.

(B) Images of cells from (A) costained for Oct4, Sox2, Sox1, and DAPI.

(C) Images of cells transfected with a constitutive Oct4 plasmid for 24 hr prior to CHIR-induced ME differentiation costained for Oct4, Brachyury, and DAPI.

(D) Scatter plot of Brachyury versus Sox2 in over 5000 cells transfected with a Sox2 plasmid 24 hr prior to the induction of mesendodermal differentiation with 200 ng/ml Wnt3a (identical results obtained with CHIR, data not shown) costained for Sox2, Brachyury, and DAPI.

(E) Images of cells from (D).

(F) Images of cells transfected with siRNA against Oct4 and a constitutive Sox2 plasmid costained for Oct4, Sox2, Brachyury, and DAPI.

(G) Images of ESCs transfected with a Brn2 plasmid and stained for Brn2 and Oct4 under pluripotency-promoting conditions.

See also Figure S5.

differentiation. As Sox2 protein levels increase, Sox2 binding increases in the *Brachyury* promoter. Thus, these two regulatory regions become enriched for either Oct4 or Sox2 during lineage choice. These results together with our imaging data suggest that Oct4 and Sox2 might perform lineage specific repression during differentiation. In such a model, Oct4 would repress the NE lineage and Sox2 the ME lineage.

Oct4 or Sox2 Perturbation Modulates Cell Fate Selection

To test the functional roles of Oct4 and Sox2 in lineage selection, we interfered with the levels of these proteins by transfecting differentiating cells with overexpression plasmids and siRNA constructs (Figure S5). In these experiments, we drove differentiation into NE or ME progenitor cells at high efficiency by adding the induction signals retinoic acid or CHIR to ESCs after 48 hr in N2B27 (see "ESCs Differentiate into Germ Layer Progenitors In Vitro"). We performed the transfection experiments without selection markers so that cells transfected with a given plasmid or siRNA occurred next to untransfected cells, and in a single field of view we could examine perturbed and unperturbed cells (Figure S5).

We confirmed that Oct4 inhibits NE differentiation by transfecting cells with a constitutively expressing Oct4 plasmid while inducing NE differentiation with retinoic acid. Cells with high Oct4 did not express Sox1, and cells expressing Sox1 had low Oct4 levels (Figure 6A and 6B), as illustrated by the "L" shape of the scatter plot (Figure 6A). In contrast, Oct4 overexpression during mesendodermal differentiation did not block Brachyury expression (Figure 6C).

We confirmed that Sox2 inhibits ME differentiation by driving constitutive expression of Sox2 during mesendodermal differentiation driven by CHIR. Cells with high Sox2 expression did not express Brachyury (Figures 6D and 6E), again highlighted by

the "L"-shaped scatter plot (Figure 6D). Further, cells in which Sox2 was driven constitutively and Oct4 expression was abrogated using siRNA did not express Brachyury (Figure 6F), showing that ME inhibition by Sox2 was independent of Oct4. Furthermore, Brachyury expression was confined to cells that retained Oct4 expression suggesting that Oct4 is necessary for mesendodermal differentiation.

Further, overexpressing Sox2 while abrogating Oct4 expression under conditions supporting pluripotency led to a fraction of cells activating the neural ectodermal regulator Sox1 (Figure S5), suggesting that Sox2 drives NE differentiation.

As another test of relevance, we asked whether forced expression of terminal lineage markers induces the observed pattern of Oct4 or Sox2 protein expression. Brn2 is a core regulator of neural identity that is induced in NE cells in our experimental system at a similar time as Sox1 (Figure S1). Forced Brn2 expression can convert fibroblasts directly into neurons (Vierbuchen et al., 2010). We found that constitutive expression of Brn2 in ESCs growing in pluripotency promoting conditions reproducibly downregulated Oct4 in these cells, as shown by images in Figure 6G.

These experiments show that Oct4 specifically represses Sox1 and the NE lineage, and Sox2 specifically represses Brachyury and the mesendodermal lineage. Thus, the differential activation of these genes critically regulates cell fate choice.

Differential Regulation of Oct4 and Sox2 Enables Signal Integration

Together, the data presented above lead us to a model of pluripotency circuit regulation during differentiation and lineage choice. In the pluripotent state, positive regulatory interactions between Oct4, Sox2, Nanog, Klf4, Klf5, and Tbx3 maintain these proteins at high and correlated levels, preventing differentiation. We verified positive regulatory interactions between Oct4, Sox2, and Nanog using siRNA (Figures S5 and S6). Upon withdrawal of pluripotency promoting factors, LIF and BMP, or with the direct abrogation of Nanog expression with siRNA, the levels of pluripotency factors fall. This fall allows the differentiation signals, Wnt and retinoic acid or FGF, to differentially regulate elements of the circuit. The differential regulation competes with the intrinsic positive interactions between the pluripotency factors. The ME inducing signals drive Sox2 levels down and Oct4 levels up, while the NE inducing signals drive Oct4 down and Sox2 up. Because Oct4 specifically inhibits the NE lineage and Sox2 specifically inhibits the ME lineage, the cells make a lineage choice.

We modeled the competition between the intrinsic positive regulation of the pluripotency factors and the differential regulation by signals. Model analysis (Extended Experimental Procedures, Figures 7B–7F, and Figures S6C and S6D) revealed that this competition allows the pluripotency circuit to perform signal integration, so that one differentiation signal can change the cell's interpretation of the other. Specifically, the model predicted that exposure of the cell to Wnt and retinoic acid simultaneously can jam the pluripotency circuit in a high Oct4 and high Sox2 state, leading to the expression of Nanog (Figure 7F) and thus preventing the activation of either Brachyury or Sox1.

To test the prediction of our model, we added combinations of RA and CHIR to differentiating ESCs and quantified the fraction of cells that activated the germ layer markers Sox1-GFP or Brachyury by microscopy. Experimentally, we found that RA changes the cell's interpretation of the CHIR signal. We added 250 nM RA to cells and titrated the concentration of CHIR. In cells treated with CHIR between 3–5 μM and 250 nM retinoic acid, we did not detect either Sox1-GFP or Brachyury staining by microscopy (Figure 7G), while cells treated with these concentrations of CHIR alone would have activated Brachyury at 70% efficiency. To ascertain the fate of these cells, we stained the same cells for Oct4, Sox2, and Nanog, and we found that many cells contained levels of these proteins similar to levels observed under pluripotency promoting conditions (Figure 7H). This implies that the cells do not enter either the ME or NE fate within the duration of the experiment. This could be because of delayed lineage choice or because the cells have entered a distinct state from which they cannot reach the ME and NE fate. A detailed analysis of the gene expression pattern, epigenetic state, and potency of these cells is the subject of future work and will give additional insight into the state of these jammed cells.

DISCUSSION

In this work, we asked how ESCs leave the pluripotent state and select between the ME and NE cell fate. As a cell transitions from ESC to germ layer progenitor, several hundred genes are downregulated. By reconstituting the lineage branch in vitro, we could classify DNA binding proteins based on their expression pattern during lineage selection. We found that very few proteins that are present in ESCs are regulated in a lineage specific fashion during differentiation providing a substantial simplification of the complex, underlying transcriptional circuit. By using the underlying lineage branch as a guide, we can identify small, crucial sets of factors that control lineage choice within the complex regulatory circuits described by genomic methods.

Through this approach, we found that pluripotency maintenance and lineage choice are intricately linked. The pluripotency circuit is known to act as a unit that strongly represses lineage specific gene expression in ESCs (Figure 1B). However, rather than being a monolithic entity, the pluripotency circuit components have lineage specific roles, so that the same proteins can also be used for lineage selection. While the intact pluripotency circuit inhibits all germ layer differentiation, Oct4 specifically represses only the neural ectodermal fate, while Sox2 specifically represses only the mesendodermal fate. Together, Oct4 and Sox2 repress differentiation into either germ layer fate. When these two proteins are differentially regulated leading to high Oct4 and low Sox2 levels, or low Oct4 and high Sox2 levels, either the mesendodermal fate or the neural ectodermal fate becomes available to the cell. Thus, by modulating the levels of the same proteins that together repress differentiation, a cell can select a germ layer fate.

Terminal markers of lineage choice, like Sox1 and Brachyury, have been identified in many progenitor cell populations. However, such terminal markers only report on the outcome of differentiation and do not allow examination of the events leading to cell fate choice. Oct4 and Sox2 protein levels provide a way to track the state of the cell continuously from ESC to NE or ME progenitor cell. By studying proteins that are present and

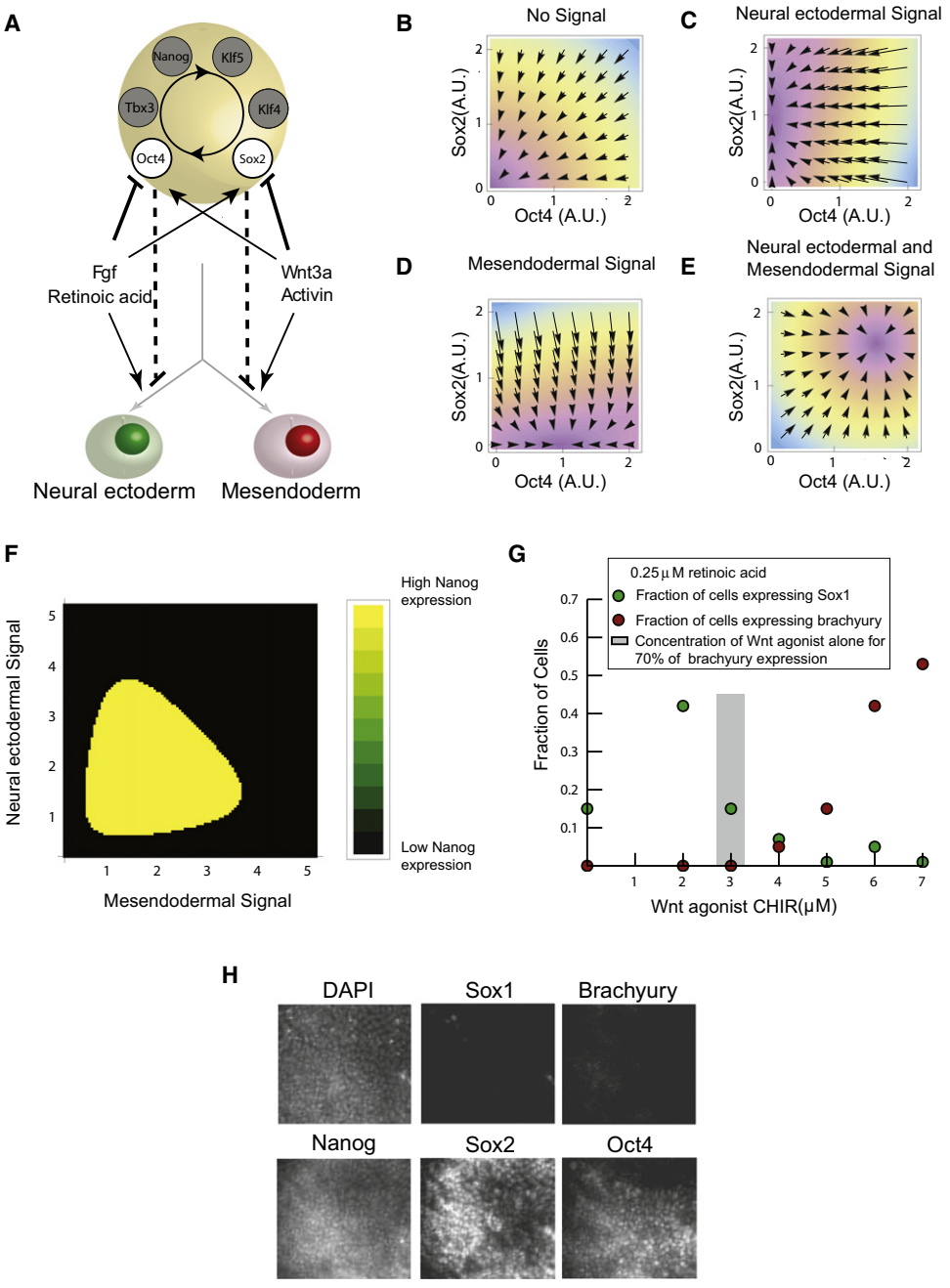

Figure 7. The Architecture of the Pluripotency Circuit Enables Signal Integration and Lineage Choice

(A) Model for the coupling between the pluripotency circuit, differentiation signals, and cell fates based upon data from Figures 3, 4 and 5. The asymmetric inhibition of Oct4 and Sox2 by differentiation signals competes with positive feedback between circuit elements (circular arrow), Oct4, Sox2, Nanog, Klf5, Klf4, and Tbx3.

(B–E) Plots of the Oct4 and Sox2 phase space showing the stable fixed points in the presence of different combinations of differentiation signals as defined by the mathematical model (Extended Experimental Procedures). In each panel, arrows depict the magnitude and direction of the time rate of change of Oct4 and Sox2 concentration in Oct4 and Sox2 space. Conditions are in the absence of differentiation signals (B), in the presence of NE inducing signals (C), in the presence of ME inducing signals (D), and in the presence of inducers of both lineages (E).

(F) Plot of steady state Nanog level for combinations of ME- and NE-inducing signals. Nanog is near zero in black regions but is present at ESC levels in yellow regions.

(G) A titration of the Wnt agonist CHIR in cells also treated with 250 nM retinoic acid. Green dots show fraction of cells activating Sox1 and red dots indicate fraction of cells activating Brachyury.

(H) Images of Sox1-GFP cells treated with 5 μM CHIR and 250 nM retinoic acid immunostained for Brachyury, Oct4, Sox2, and Nanog.

See also Figure S6.

modulated continuously during lineage selection, we gain access to the detailed dynamics of the process. For example, sorting cells by their Oct4 or Sox2 levels during the cell fate transition would enable examination of epigenetic regulation and transcription factor binding patterns as a function of the cell's differentiation status. Having continuous markers of lineage selection can thus illuminate the temporal coordination of a broad array of cellular processes and their impact on a cell's developmental decision.

In many systems, a progenitor cell's response to differentiation signals depends on the cell's history, its context, and the presence of other signals in the environment. For example, in the developing limb bud, FGF and Wnt signals together retain progenitor cells in a multipotent state but individually promote differentiation and cell lineage specification (Hu et al., 2009; ten Berge et al., 2008a). Our study demonstrates that a context-dependent interpretation of the signals can arise in part from the architecture of the transcriptional circuit that governs the multipotent state. External signals differentially activate Oct4 and Sox2, so that conflicting signals alter the cell's interpretation of one another through their combined influence on the pluripotency circuit dynamics as seen in Figure 7.

Core circuits of transcription factors also operate in neural progenitor cells (Briscoe et al., 2000) and hematopoietic progenitor cells (Cantor and Orkin, 2001). These circuits might also play a role in signal integration and cell fate choice. While each type of progenitor cell might use a different combination of transcription factors to make lineage choices, circuits that make developmental decisions might use similar principles to integrate information from external signals and select a fate (Anderson, 2001). Our study provides a general approach for isolating decision-making circuits and for relating broad scale circuit structure to the dynamic behavior of single cells.

EXPERIMENTAL PROCEDURES

ESC Culture and Differentiation Assays

Cells were propagated in feeder-free, serum-free N2B27 media supplemented with LIF and BMP as described previously (Ying and Smith, 2003; Ying et al., 2008). ESC media was supplemented with the FGF receptor inhibitor PD173074 (Sigma, StemGent) at 100 nM to suppress background differentiation. For differentiation toward the neural ectoderm or mesendoderm lineages, ESCs were plated into N2B27 for 48 hr, followed by addition of Wnt3a (200 ng/ml) or CHIR99021 (3 μM) for ME differentiation (ten Berge et al., 2008b) or RA (500 nM) for NE differentiation (Ying et al., 2003b). For differentiation experiments, cells were immunostained 36 hr after addition of the differentiation signal.

Immunofluorescence and FACS

Immunofluorescence and flow cytometry were performed via standard techniques (Extended Experimental Procedures).

Live-Cell Fluorescence Microscopy

Cells were seeded on glass bottom dishes (MatTek) and imaged on an environmentally enclosed Zeiss Axiovision.

Analysis of Published Microarray and ChIP-Seq Data

Transcription factors and DNA binding proteins in ESCs, ME cells, and NE cells were identified from GEO GSE12982 (Shen et al., 2008). Published ChIP-seq data (Chen et al., 2008; Marson et al., 2008) were analyzed with custom code in Mathematica (Wolfram) (Extended Experimental Procedures).

Gene Expression Microarray for ES versus 48 hr state

Microarrays were conducted in triplicates on Illumina Mouse-Ref8 BeadChips, according to the manufacturer's protocol. Quantile normalization was used in Figure 2B.

Overexpression and siRNA Knockdown

Overexpression experiments used CAG promoter-driven Oct4 and Sox2 plasmids (Mitsui et al., 2003). siRNA constructs were validated in previous studies (Hu et al., 2009). Plasmid and/or siRNA transfections were performed 24 hr before addition of differentiation signals.

Generation of Oct4-mCitrine Transgenic ESC Line

Oct4-mCitrine fusion construct was generated with Red/ET Recombination (Gene Bridges). The construct consisted of the distal and proximal enhancers of *Oct4*, the *Oct4* open reading frame, the linker, mCitrine cDNA, the native 3′ untranslated region of *Oct4*, and the loxP-PGK-gb2-neo-loxP selection cassette (Gene Bridges).

Chromatin Immunoprecipitation and qPCR

Chromatin immunoprecipitation (ChIP) was performed essentially according to Mikkelsen et al. (2007). qPCR was performed on an ABI 7900HT with primers from ChIP-qPCR tiling arrays (SABiosciences) and custom primer sets (Operon) (Table S1). Fold enrichment was calculated relative to input.

Mathematical Modeling of Pluripotency Circuit

Simulation of mathematical models was performed using custom written code in MATLAB (MathWorks) (Extended Experimental Procedures).

ACCESSION NUMBERS

Microarray data are available in the Gene Expression Omnibus (GEO) database (http://www.ncbi.nlm.nih.gov/geo/) under the accession number GSE29005.

SUPPLEMENTAL INFORMATION

Supplemental Information includes Extended Experimental Procedures, six figures, and one table and can be found with this article online at doi:10.1016/j.cell.2011.05.017.

ACKNOWLEDGMENTS

We thank Doug Melton, Sean Eddy, Areez Mody, and Alexander Schier for scientific discussions and Rene Maehr, Masa Yamagata, and Dawen Cai for discussions and technical assistance. We thank Manfred Baetscher and the Harvard Genome Modification Facility for assistance with the cell line generation. We thank Bodo Stern, Nicole Francis, and in particular Sean Eddy and three anonymous referees for extensive comments on the manuscript. We thank the Harvard Stem Cell Institute Seed Grant (S.R.) and the Massachusetts Life Science Center (A.M.) for support. Microarray hybridization and measurements were performed by the Molecular Genetics Core Facility at Children's Hospital Boston supported by NIH-P50-NS40828, and NIH-P30-HD18655. M.T. and S.R. conceived the project. M.T. established the experimental system and performed the immunofluorescence and perturbation experiments. S.J.L. and M.T. built the cell lines and performed microarray experiments. L.N.Z. performed the FACS experiments and established techniques for long term microscopy of ESCs on glass. M.T. and S.J.L. performed the time-lapse microscopy experiments. Z.S. and A.M. did the ChIP for Oct4 and Sox2. S.J.L., M.T., and S.R. performed the tiling qPCR experiments. M.T., S.R., and S.J.L. performed the data and mathematical analyses and wrote the manuscript.

Received: October 15, 2010
Revised: March 3, 2011
Accepted: May 16, 2011
Published: June 9, 2011

REFERENCES

Abranches, E., Silva, M., Pradier, L., Schulz, H., Hummel, O., Henrique, D., and Bekman, E. (2009). Neural differentiation of embryonic stem cells in vitro: a road map to neurogenesis in the embryo. PLoS ONE *4*, e6286.

Anderson, D.J. (2001). Stem cells and pattern formation in the nervous system: the possible versus the actual. Neuron *30*, 19–35.

Briscoe, J., Pierani, A., Jessell, T.M., and Ericson, J. (2000). A homeodomain protein code specifies progenitor cell identity and neuronal fate in the ventral neural tube. Cell *101*, 435–445.

Cantor, A.B., and Orkin, S.H. (2001). Hematopoietic development: a balancing act. Curr. Opin. Genet. Dev. *11*, 513–519.

Chen, X., Xu, H., Yuan, P., Fang, F., Huss, M., Vega, V.B., Wong, E., Orlov, Y.L., Zhang, W., Jiang, J., et al. (2008). Integration of external signaling pathways with the core transcriptional network in embryonic stem cells. Cell *133*, 1106–1117.

Chew, J.L., Loh, Y.H., Zhang, W., Chen, X., Tam, W.L., Yeap, L.S., Li, P., Ang, Y.S., Lim, B., Robson, P., and Ng, H.H. (2005). Reciprocal transcriptional regulation of Pou5f1 and Sox2 via the Oct4/Sox2 complex in embryonic stem cells. Mol. Cell. Biol. *25*, 6031–6046.

Davidson, E.H., Rast, J.P., Oliveri, P., Ransick, A., Calestani, C., Yuh, C.H., Minokawa, T., Amore, G., Hinman, V., Arenas-Mena, C., et al. (2002). A genomic regulatory network for development. Science *295*, 1669–1678.

Ema, M., Mori, D., Niwa, H., Hasegawa, Y., Yamanaka, Y., Hitoshi, S., Mimura, J., Kawabe, Y., Hosoya, T., Morita, M., et al. (2008). Krüppel-like factor 5 is essential for blastocyst development and the normal self-renewal of mouse ESCs. Cell Stem Cell *3*, 555–567.

Greber, B., Wu, G., Bernemann, C., Joo, J.Y., Han, D.W., Ko, K., Tapia, N., Sabour, D., Sterneckert, J., Tesar, P., and Schöler, H.R. (2010). Conserved and divergent roles of FGF signaling in mouse epiblast stem cells and human embryonic stem cells. Cell Stem Cell *6*, 215–226.

Han, J., Yuan, P., Yang, H., Zhang, J., Soh, B.S., Li, P., Lim, S.L., Cao, S., Tay, J., Orlov, Y.L., et al. (2010). Tbx3 improves the germ-line competency of induced pluripotent stem cells. Nature *463*, 1096–1100.

Hu, G., Kim, J., Xu, Q., Leng, Y., Orkin, S.H., and Elledge, S.J. (2009). A genome-wide RNAi screen identifies a new transcriptional module required for self-renewal. Genes Dev. *23*, 837–848.

Ivanova, N., Dobrin, R., Lu, R., Kotenko, I., Levorse, J., DeCoste, C., Schafer, X., Lun, Y., and Lemischka, I.R. (2006). Dissecting self-renewal in stem cells with RNA interference. Nature *442*, 533–538.

Jackson, S.A., Schiesser, J., Stanley, E.G., and Elefanty, A.G. (2010). Differentiating embryonic stem cells pass through 'temporal windows' that mark responsiveness to exogenous and paracrine mesendoderm inducing signals. PLoS ONE *5*, e10706.

Jiang, J., Chan, Y.S., Loh, Y.H., Cai, J., Tong, G.Q., Lim, C.A., Robson, P., Zhong, S., and Ng, H.H. (2008). A core Klf circuitry regulates self-renewal of embryonic stem cells. Nat. Cell Biol. *10*, 353–360.

Kim, J.B., Zaehres, H., Wu, G., Gentile, L., Ko, K., Sebastiano, V., Araúzo-Bravo, M.J., Ruau, D., Han, D.W., Zenke, M., and Schöler, H.R. (2008). Pluripotent stem cells induced from adult neural stem cells by reprogramming with two factors. Nature *454*, 646–650.

Li, J.Y., Pu, M.T., Hirasawa, R., Li, B.Z., Huang, Y.N., Zeng, R., Jing, N.H., Chen, T., Li, E., Sasaki, H., and Xu, G.L. (2007). Synergistic function of DNA methyltransferases Dnmt3a and Dnmt3b in the methylation of Oct4 and Nanog. Mol. Cell. Biol. *27*, 8748–8759.

Lu, R., Markowetz, F., Unwin, R.D., Leek, J.T., Airoldi, E.M., MacArthur, B.D., Lachmann, A., Rozov, R., Ma'ayan, A., Boyer, L.A., et al. (2009). Systems-level dynamic analyses of fate change in murine embryonic stem cells. Nature *462*, 358–362.

Marson, A., Levine, S.S., Cole, M.F., Frampton, G.M., Brambrink, T., Johnstone, S., Guenther, M.G., Johnston, W.K., Wernig, M., Newman, J., et al. (2008). Connecting microRNA genes to the core transcriptional regulatory circuitry of embryonic stem cells. Cell *134*, 521–533.

Masui, S., Nakatake, Y., Toyooka, Y., Shimosato, D., Yagi, R., Takahashi, K., Okochi, H., Okuda, A., Matoba, R., Sharov, A.A., et al. (2007). Pluripotency governed by Sox2 via regulation of Oct3/4 expression in mouse embryonic stem cells. Nat. Cell Biol. *9*, 625–635.

Masui, S., Ohtsuka, S., Yagi, R., Takahashi, K., Ko, M.S., and Niwa, H. (2008). Rex1/Zfp42 is dispensable for pluripotency in mouse ES cells. BMC Dev. Biol. *8*, 45.

Mikkelsen, T.S., Ku, M., Jaffe, D.B., Issac, B., Lieberman, E., Giannoukos, G., Alvarez, P., Brockman, W., Kim, T.K., Koche, R.P., et al. (2007). Genome-wide maps of chromatin state in pluripotent and lineage-committed cells. Nature *448*, 553–560.

Mitsui, K., Tokuzawa, Y., Itoh, H., Segawa, K., Murakami, M., Takahashi, K., Maruyama, M., Maeda, M., and Yamanaka, S. (2003). The homeoprotein Nanog is required for maintenance of pluripotency in mouse epiblast and ES cells. Cell *113*, 631–642.

Miyagi, S., Nishimoto, M., Saito, T., Ninomiya, M., Sawamoto, K., Okano, H., Muramatsu, M., Oguro, H., Iwama, A., and Okuda, A. (2006). The Sox2 regulatory region 2 functions as a neural stem cell-specific enhancer in the telencephalon. J. Biol. Chem. *281*, 13374–13381.

Nishikawa, S., Jakt, L.M., and Era, T. (2007). Embryonic stem-cell culture as a tool for developmental cell biology. Nat. Rev. Mol. Cell Biol. *8*, 502–507.

Niwa, H. (2007). How is pluripotency determined and maintained? Development *134*, 635–646.

Niwa, H. (2010). Mouse ES cell culture system as a model of development. Dev. Growth Differ. *52*, 275–283.

Niwa, H., Miyazaki, J., and Smith, A.G. (2000). Quantitative expression of Oct-3/4 defines differentiation, dedifferentiation or self-renewal of ES cells. Nat. Genet. *24*, 372–376.

Novershtern, N., Subramanian, A., Lawton, L.N., Mak, R.H., Haining, W.N., McConkey, M.E., Habib, N., Yosef, N., Chang, C.Y., Shay, T., et al. (2011). Densely interconnected transcriptional circuits control cell states in human hematopoiesis. Cell *144*, 296–309.

Odom, D.T., Zizlsperger, N., Gordon, D.B., Bell, G.W., Rinaldi, N.J., Murray, H.L., Volkert, T.L., Schreiber, J., Rolfe, P.A., Gifford, D.K., et al. (2004). Control of pancreas and liver gene expression by HNF transcription factors. Science *303*, 1378–1381.

Pasini, D., Cloos, P.A., Walfridsson, J., Olsson, L., Bukowski, J.P., Johansen, J.V., Bak, M., Tommerup, N., Rappsilber, J., and Helin, K. (2010). JARID2 regulates binding of the Polycomb repressive complex 2 to target genes in ES cells. Nature *464*, 306–310.

Peng, J.C., Valouev, A., Swigut, T., Zhang, J., Zhao, Y., Sidow, A., and Wysocka, J. (2009). Jarid2/Jumonji coordinates control of PRC2 enzymatic activity and target gene occupancy in pluripotent cells. Cell *139*, 1290–1302.

Sachs, K., Perez, O., Pe'er, D., Lauffenburger, D.A., and Nolan, G.P. (2005). Causal protein-signaling networks derived from multiparameter single-cell data. Science *308*, 523–529.

Sato, N., Meijer, L., Skaltsounis, L., Greengard, P., and Brivanlou, A.H. (2004). Maintenance of pluripotency in human and mouse embryonic stem cells through activation of Wnt signaling by a pharmacological GSK-3-specific inhibitor. Nat. Med. *10*, 55–63.

Schuettengruber, B., and Cavalli, G. (2009). Recruitment of polycomb group complexes and their role in the dynamic regulation of cell fate choice. Development *136*, 3531–3542.

Shen, X., Liu, Y., Hsu, Y.J., Fujiwara, Y., Kim, J., Mao, X., Yuan, G.C., and Orkin, S.H. (2008). EZH1 mediates methylation on histone H3 lysine 27 and complements EZH2 in maintaining stem cell identity and executing pluripotency. Mol. Cell *32*, 491–502.

Sikorska, M., Sandhu, J.K., Deb-Rinker, P., Jezierski, A., Leblanc, J., Charlebois, C., Ribecco-Lutkiewicz, M., Bani-Yaghoub, M., and Walker, P.R. (2008). Epigenetic modifications of SOX2 enhancers, SRR1 and SRR2, correlate with in vitro neural differentiation. J. Neurosci. Res. *86*, 1680–1693.

Silva, J., and Smith, A. (2008). Capturing pluripotency. Cell *132*, 532–536.

Takahashi, K., and Yamanaka, S. (2006). Induction of pluripotent stem cells from mouse embryonic and adult fibroblast cultures by defined factors. Cell *126*, 663–676.

ten Berge, D., Brugmann, S.A., Helms, J.A., and Nusse, R. (2008a). Wnt and FGF signals interact to coordinate growth with cell fate specification during limb development. Development *135*, 3247–3257.

ten Berge, D., Koole, W., Fuerer, C., Fish, M., Eroglu, E., and Nusse, R. (2008b). Wnt signaling mediates self-organization and axis formation in embryoid bodies. Cell Stem Cell *3*, 508–518.

Tesar, P.J., Chenoweth, J.G., Brook, F.A., Davies, T.J., Evans, E.P., Mack, D.L., Gardner, R.L., and McKay, R.D. (2007). New cell lines from mouse epiblast share defining features with human embryonic stem cells. Nature *448*, 196–199.

Tomioka, M., Nishimoto, M., Miyagi, S., Katayanagi, T., Fukui, N., Niwa, H., Muramatsu, M., and Okuda, A. (2002). Identification of Sox-2 regulatory region which is under the control of Oct-3/4-Sox-2 complex. Nucleic Acids Res. *30*, 3202–3213.

Vierbuchen, T., Ostermeier, A., Pang, Z.P., Kokubu, Y., Südhof, T.C., and Wernig, M. (2010). Direct conversion of fibroblasts to functional neurons by defined factors. Nature *463*, 1035–1041.

Wang, J., Rao, S., Chu, J., Shen, X., Levasseur, D.N., Theunissen, T.W., and Orkin, S.H. (2006). A protein interaction network for pluripotency of embryonic stem cells. Nature *444*, 364–368.

Yamaguchi, T.P., Takada, S., Yoshikawa, Y., Wu, N., and McMahon, A.P. (1999). T (Brachyury) is a direct target of Wnt3a during paraxial mesoderm specification. Genes Dev. *13*, 3185–3190.

Ying, Q.L., and Smith, A.G. (2003). Defined conditions for neural commitment and differentiation. Methods Enzymol. *365*, 327–341.

Ying, Q.L., Nichols, J., Chambers, I., and Smith, A. (2003a). BMP induction of Id proteins suppresses differentiation and sustains embryonic stem cell self-renewal in collaboration with STAT3. Cell *115*, 281–292.

Ying, Q.L., Stavridis, M., Griffiths, D., Li, M., and Smith, A. (2003b). Conversion of embryonic stem cells into neuroectodermal precursors in adherent monoculture. Nat. Biotechnol. *21*, 183–186.

Ying, Q.L., Wray, J., Nichols, J., Batlle-Morera, L., Doble, B., Woodgett, J., Cohen, P., and Smith, A. (2008). The ground state of embryonic stem cell self-renewal. Nature *453*, 519–523.